Journal of Computational Applied Mechanics 2021, 52(2): 246-255
DOI: 10.22059/jcamech.2021.315459.578

RESEARCH PAPER

Effects of Annulus Geometry and Liquid Properties on the Well Conditions during UBD Operation

Saeed Ghobadpouri [1, *], *Iman Zamani* [2], *Ali Falavand Jozaei* [3]

[1] *Mechanical Engineering Department, Faculty of Gas and Petroleum, Yasouj University, Gachsaran, Iran*
[2] *Electrical and Electronic Engineering Department, Shahed University, Tehran, Iran*
[3] *Department of Mechanical Engineering, Ahvaz Branch, Islamic Azad University, Ahvaz, Iran*

Abstract
Well conditions during drilling operation can be predicted using numerical simulation. During under-balanced drilling (UBD) operation, controlling the bottom-hole pressure (BHP) in a suitable range and also appropriate hole-cleaning is essential. In this paper, numerical simulation of gas-liquid-solid three-phase flow in the annulus is used to study the effects of annulus geometry and also liquid properties on the BHP and hole-cleaning during UBD operation. To validate the numerical simulation, the results are compared with the experimental data from a laboratory study. Also, the gain results from developed code are compared with the actual field data from a real well, several mechanistic models from WellFlo software, and gas- liquid two- fluid numerical simulation. Due to the significance of controlling the BHP and hole-cleaning during UBD operation, the effects of annulus geometry and liquid phase properties on BHP and the solid volume fraction distribution are investigated. According to the results, changing the hydraulic diameter and cross-sectional area of the annulus can affect BHP and hole- cleaning in UBD operation. In other words, increasing the hydraulic diameter at a constant cross- sectional area improves hole-cleaning and decrease BHP. Also, decreasing the cross-sectional area at a constant hydraulic diameter improves hole-cleaning and increase BHP. The results show that the liquid viscosity affects hole-cleaning through two contrary mechanisms. In fact, by increasing the liquid viscosity, carrying capacity of the liquid phase is increased and cutting transfer velocity is decreased.

Keywords: Under-Balanced Drilling, Bottom-Hole Pressure, Hole-Cleaning, Geometrical Parameters, Liquid Properties

Introduction and Problem Statement

Drilling operation techniques are defined based on the comparison of bottom-hole pressure (BHP) and reservoir pressure. If BHP is maintained lower than the reservoir pressure, then the drilling technique is called under-balanced drilling (UBD), and if BHP is greater than the reservoir pressure then the drilling technique is over-balanced drilling (OBD). During UBD operation, gas-liquid two-phase flow is injected from the wellhead to the drill string. At the bottom hole, drill cuttings add to this two-phase flow. Therefore, in the annulus, gas-liquid-solid three-phase fluid is flowing from the bottom to the wellhead. Predicting and controlling the BHP in a suitable range and also proper cutting transport in the annulus are the main challenges during UBD operation.

Much of the research in UBD is focused on predicting the effects of different parameters on the pressure distribution and cutting volume fraction distribution. For this purpose, Guo et al. [1] developed a mechanistic model to simulate gas-liquid two-phase flow in UBD operation regardless of the solid particle and the velocity difference between gas and liquid phases. They

* Corresponding author , E-mail addresses: sghy_790@yahoo.com , ghobadpouri.s@yu.ac.ir
Tel.: 0098(74)3100-1000 Fax: 0098(74)3100-1000

calculated the optimal airflow rate in order to increase the rate of penetration. Fan et al. [2] developed a computer program for predicting the behavior of multi-phase fluid flow during UBD operation. This program is able to consider the flow of oil, gas, water, and drilling fluid simultaneously, but the effects of solid-phase were not considered. Lage [3] and Lage and Time [4] simulated the upward gas-liquid two-phase flow in concentric annuli based on a new mechanistic model. They have validated the results using the data of a real well. Guo and Ghalambor [5], by considering the effect of solid phase and using a mechanistic approach, determined the acceptable range of injected liquid and gas phases to ensure that BHP being in the range between formation pressure and blow out pressure and also drill cuttings are appropriately transported. Perez-Tellez [6] and Perez-Tellez et al. [7] assumed that in the annulus, the gas-liquid two-phase are flows and neglected from solid particles. They proposed a mechanistic model to predict standpipe pressure and BHP in various flow patterns. They developed a numerical method based on the drift flux model for simulating the transient two-phase flow in the vertical annuls in the UBD operation. Fadairo et al. [8] has studied the effects of the solid volume fraction on the pressure drop in a vertical tube mechanistically. Yan et al. [9] had an overview of the empirical correlations, sensitivity analyses, and mechanical models for cuttings transport with aerated liquid and foam. The conclusion of this article stated that despite significant improvements that have been achieved in the past several decades, but more researches will be conducted to more understand the cuttings transport mechanism. Khezrian et al. [10] simulated the gas-liquid two-phase flow in UBD operation by using a one-dimensional form of the steady-state two-fluid model in the Eulerian frame of reference. They did not consider the effect of the solid phase. Gas-liquid two-phase flow in the annulus of a well with actual dimensions during UBD operations with the effect of temperature variation due to heat transfer of drilling fluids with the formation was studied by Hajidavalloo et al. [11]. In this research, the effects of cuttings are not considered and hole cleaning problems not investigated. Li et al. [12] established a prediction model based on the dynamic bottom hole pressure balance to predict the horizontal well's maximum allowable measured depth during UBD operation. In this study, the pore pressure is taken as the critical point at which horizontal wells must stop extending to maintain the under-balanced state of the bottom hole. The hole-cleaning problems were not considered in this study.

The literature review shows that most of the previous researches in the UBD operation focused on the study of the effects of operational parameters such as injected gas and liquid flow rate on BHP. Meanwhile, the geometry of the annulus and fluid properties influences hole-cleaning and BHP and plays a very important role in the designs of successful UBD operations. To the author's best knowledge, no papers have focused on the effects of annulus geometry and liquid properties on BHP and cutting transport during the UBD operation.

In this paper, the numerical simulation of the gas-liquid-solid three-phase flow during under-balanced drilling operation is used to investigate the effects of annulus geometry and liquid viscosity and density on the BHP and cutting transport. Therefore, in the following sections, the governing equations of the multi-fluid model, corresponding relations, the numerical method, and solution algorithm are presented, respectively. The simulation is validated by a laboratory study and also by field data from a real well. The effects of geometry parameters such as hydraulic diameter, cross-sectional area on BHP, and cutting transport are discussed. Finally, the effects of viscosity and density of the liquid phase on BHP and cutting transport are investigated.

Governing equations

In this paper, one-dimensional form of the steady-state, multi-fluid model in the Eulerian frame of reference is used to simulate gas-liquid-solid three-phase flow in the annulus. The mass

transfer between phases was neglected, and the temperature gradient along the well follows the geothermal gradient. Here, it is assumed that the gas phase is to be compressible, and the liquid is incompressible. Considering these assumptions, the governing equations consist of continuities, and momentum equations for each phase are as follows (Evje and Flatten [13], Hatta et al. [14])

$$\frac{d}{dx}\left(\alpha_G \rho_G u_G A\right)=0 \tag{1}$$

$$\frac{d}{dx}\left(\alpha_L \rho_L u_L A\right)=0 \tag{2}$$

$$\frac{d}{dx}\left(\alpha_S \rho_S u_S A\right)=0 \tag{3}$$

$$\frac{d}{dx}\left(\alpha_G \rho_G u_G^2 A\right)=-A\left(F_{iG}+F_{wG}+F_{gG}+F_{vG}+\alpha_G \frac{\partial P}{\partial x}\right)-\Delta P_{iG}\frac{d\left(A\alpha_G\right)}{dx} \tag{4}$$

$$\frac{d}{dx}\left(\alpha_L \rho_L u_L^2 A\right)=-A\left(F_{iL}+F_{wL}+F_{gL}+F_{vL}+\alpha_L \frac{\partial P}{\partial x}\right)-\Delta P_{iL}\frac{d\left(A\alpha_L\right)}{dx} \tag{5}$$

$$\frac{d}{dx}\left(\alpha_S \rho_S u_S^2 A\right)=-A\left(F_{iS}+F_{wS}+F_{gS}+F_{vS}+\alpha_S \frac{\partial P}{\partial x}\right) \tag{6}$$

In the above-mentioned equations, α denotes the volume fractions, ρ is density, u is the velocity, and A is cross-sectional area. The G, L, and S subscripts refer to the gas, liquid, and the solid phases, respectively. Also, F_g is the gravitational force and F_v is virtual mass force. F_i denotes the interface shear force and F_w is the wall shear force. ΔP is the pressure correction term. Modeling of the above-mentioned forces and also pressure correction term can be found in Hatta et al. [14].

In addition to the conservative equations of mass and momentum, two other equations are needed to close the system. These equations are saturation constraint equation and the gas equation of state. The saturation constraint equation states that

$$\sum_K \alpha_K = \alpha_G + \alpha_L + \alpha_S = 1 \tag{7}$$

And the equation of state for the gas phase is as follows

$$\rho_G = \rho_G\left(P_G, T_G\right)=\frac{M_G.P}{8314.Z.T} \tag{8}$$

To calculate the compressibility factor in Equation 8, Equation 9 which is utilized by Dranchuk and Abu-Kassem [15] is used

$$Z=\left(0.3265-\frac{1.0700}{T_{\mathrm{Pr}}}-\frac{0.5339}{T_{\mathrm{Pr}}^3}+\frac{0.01569}{T_{\mathrm{Pr}}^4}-\frac{0.05165}{T_{\mathrm{Pr}}^5}\right)\rho_r+\left(0.5475-\frac{0.7361}{T_{\mathrm{Pr}}}+\frac{0.1844}{T_{\mathrm{Pr}}^3}\right)\rho_r^2$$
$$-0.1056\left(-\frac{0.7361}{T_{\mathrm{Pr}}}+\frac{0.1844}{T_{\mathrm{Pr}}^3}\right)\rho_r^5+0.6134\left(1.0+0.7210\rho_r^2\right)\frac{\rho_r^2}{T_{\mathrm{Pr}}^3}\exp\left(-0.7210\rho_r^2\right)+1.0 \tag{9}$$

In Equation 9, T_{Pr}, ρ_{Pr} are reduced temperature and reduced density, respectively.

Numerical simulation method

Continuity and momentum equations besides saturation constraint equation of the volume fractions of the phases and gas equation of state form a coupled system of ordinary differential equations with eight equations. By using the first-order approximation for the spatial derivatives, the governing equations will be changed to a coupled nonlinear algebraic system of equations. A matrix based on the governing equation defined as follows (Bratland [16].)

$$F=\begin{bmatrix}F_1\\F_2\\F_3\\F_4\\F_5\\F_6\\F_7\\F_8\end{bmatrix}=\begin{bmatrix}\left(\alpha_G\rho_G u_G A\right)_i-K_{Gin}\\ \left(\alpha_L\rho_L u_L A\right)_i-K_{Lin}\\ \left(\alpha_S\rho_S u_S A\right)_i-K_{Sin}\\ K_{Gin}\left(u_{G,i+1}-u_{G,i}\right)+\alpha_{G,i}A_i\left(P_{i+1}-P_i\right)+A\Delta P_{iG}\left(\alpha_{G,i+1}-\alpha_{G,i}\right)-\Delta X.A_i.S_{G,i}\\ K_{Lin}\left(u_{L,i+1}-u_{L,i}\right)+\alpha_{L,i}A_i\left(P_{i+1}-P_i\right)+A\Delta P_{iL}\left(\alpha_{L,i+1}-\alpha_{L,i}\right)-\Delta X.A_i.S_{L,i}\\ K_{Sin}\left(u_{S,i+1}-u_{S,i}\right)+\alpha_{S,i}A_i\left(P_{i+1}-P_i\right)-\Delta X.A_i.S_{S,i}\\ \alpha_G+\alpha_L+\alpha_S-1.0\\ \rho_{G,i}-\rho\left(P_i,T_i\right)\end{bmatrix}=\begin{bmatrix}0\\0\\0\\0\\0\\0\\0\\0\end{bmatrix} \tag{10}$$

The independent variables are all the fractions (three variables), the velocities (three variables), the gas density (one variable), and the pressure (one variable), eight variables in total. So the variables we seek to determine are:

$$Y=\begin{bmatrix}y_1 & y_2 & y_3 & y_4 & y_5 & y_6 & y_7 & y_8\end{bmatrix}^T=\begin{bmatrix}\alpha_G & \alpha_L & \alpha_S & u_G & u_L & u_S & \rho_G & P\end{bmatrix}^T \tag{11}$$

The solution method that has been used is Newton's method that details of which to solve a stratified two-phase flow described by Bratland [16]. Newton-iteration on Equations (10) and (11) is straightforward

$$Y_{n+1}=Y_n-J^{-1}F_n\left(Y_n\right) \tag{12}$$

The calculation starts from the top of the annulus by inserting everything we know at the outlet into y-vector. The choke pressure is directly inserted as P_{out}. The gas density can be obtained using the gas equation of state and choke pressure and also the temperature at the wellhead according to Equations (8) and (9). We need to guess values for α_G and α_S at the wellhead node and then setting $\alpha_L=1.0-\alpha_G-\alpha_S$. Next, determine starting values for the velocities at the wellhead in such a way that they satisfy the phase mass flow rates. Therefore, all values in Y at the outlet of the annulus are thereby known. We index the y-vector at the outlet Y_{i+1} so the second cell from wellhead becomes Y_i. All of the parameters of three-phase flow in the second cell from wellhead Y_i are guessed. These values of Y_i and Y_{i+1} are used to determine the F-vector in Equation 10. The Jacobi-matrix $J=\partial F/\partial Y$ is calculated by investigating how that affects F with slightly varying of each argument Bratland (2010). According to Equation 12, Newton-iteration processes to calculate the modified values of Y_i vector are repeated until the convergence criteria is satisfied. The convergence is achieved when $\sqrt{\sum_{i=1}^{8}F_i^2}\le 10^{-7}$. The process is repeated throughout the annulus to achieve BHP. In order to modify poor initial guesses of the first point and to go to be more accurate, the initial guess at the wellhead node is corrected by extrapolation of the first five points at the top of the annulus. Repeat the process solution from the wellhead until satisfied the convergence criteria which represented as follows $\left(\left|\alpha_{G,i=1}^{n+1}-\alpha_{G,i=1}^{n}\right|+\left|\alpha_{L,i=1}^{n+1}-\alpha_{L,i=1}^{n}\right|+\left|\alpha_{S,i=1}^{n+1}-\alpha_{S,i=1}^{n}\right|\right)\le 10^{-5}$

Results and discussion

To validate the performance of the multi-fluid model, a laboratory study by Lage and Time [4] is simulated. In this study, the well was 1275-meter-deep, and four temperature sensors and four pressure sensors are installed along with the annular space at depths of 240, 494, 998, and 1273 meters. The inner diameter of the annular space in the total length of the well is 88.9 mm, and the outer diameter is 159.4 mm. The results were obtained for water injection with 0.15 m3/min flow rate, nitrogen with 28.13 m3/min, and choke pressure 0.41 MPa. Figure (1) shows the annulus pressure variation comparisons for the laboratory study by the Lage and Time and Multi-fluid models. This figure confirms the validity of the current study.

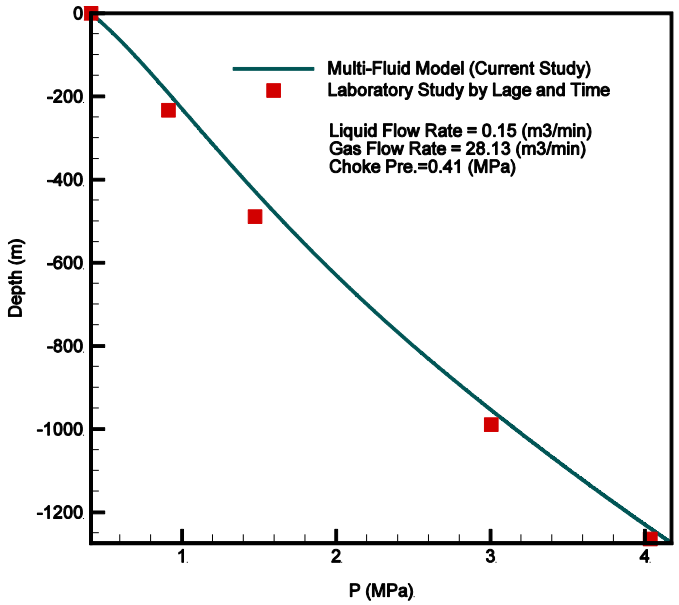

Figure 1. Pressure distribution in the annulus of laboratory study by Lage and Time

Gas-liquid-solid three-phase flow in the annulus of Muspac-53 well (Perez-Tellez [6]), which was drilled in Mexico, also confirms the validity of the current study. This well was drilled from 2597 m (8520 ft) to 2686 m (8812 ft) by means of the UBD technique. The BHP was measured and reported. During the UBD operation, the simultaneous injection of nitrogen at 15.014 m3/min (530 scf/min) and a mud with 0.94 specific gravity at 0.5075 m3/min (133 gpm) was implemented. At the wellhead, the choke pressure was set at 0.310 MPa (45.12 psi), and the temperature is 301.15 k. The temperature gradient along the annulus is 2.83 K/100m. Drilling velocity is 6 m/hour. The average cutting size supposed to be 6 mm, and the solid density is 2800 kg/m3. Annular well geometry is shown in Table 1.

Table 1. Annular well geometry

Depth (m)	Drill string outer diameter (mm)	Annuls outer diameter (mm)
0-2555	88.9	152.5
2555-2597	120.7	152.5
2597-2605	120.7	149.2

Table 2 shows the BHP, which were obtained using the multi-fluid model, field data and the result of WellFlo software (Kezrian et al. [10]) , which uses different mechanistic models such as Biggs & Brill, Hasan & Kabir, and OLGAS and also gas-liquid two-fluid model. As shown in Table 2, the gas-liquid-solid three-phase flow model yields relatively more accurate BHP than Biggs & Brill and OLGAS models of WellFlo software, but it has a little more error in comparison with the Hassan and Kabir model. The WellFlo-Hassan & Kabir model is a mechanistic model that does not provide any information about the distribution of the solid volume fraction along with the annular space.

Table 2. Comparison of BHP of Muspac-53

Model	BHP (MPa)	% Error
Field data	23.57	-
Two-Fluid Model	19.67	16.55
WellFlo-OLGAS	16.95	28.09
WellFlo-Biggs&Brill	17.76	24.65
WellFlo-Hasan & Kabir	21.14	10.31
Multi-Fluid Model (Current Study)	20.24	14.13

Effects of geometry parameters

During UBD operation, liquid and gas phases are injected from wellhead to the drill string. After passing through the drill string and bit, these fluids carry drill cutting from the bottom-hole and flows upward through the annular space between the outer wall of the drill string and formation wall. The geometry of annular space can affect BHP and hole-cleaning. Hydraulic diameter and cross-sectional area, are two important geometric parameters in annular geometry. For annular geometry, the cross-sectional area is defined as $A=\pi\left(D_{out}^2-D_{in}^2\right)$, and the hydraulic diameter is $D_h=D_{out}-D_{in}$. So, as follows, the effects of theses geometrical parameters on BHP and cutting transport are investigated.

The effects of hydraulic diameter and cross-sectional area on the BHP are presented in Figure (2) for the Muspac-53 case study. Assumed that, annular space of this well does not have any abrupt changes, and annular space has a uniform cross-sectional area. BHP has been gained from developed code for three different cross-sectional areas at various hydraulic diameters, as seen in figure (2).

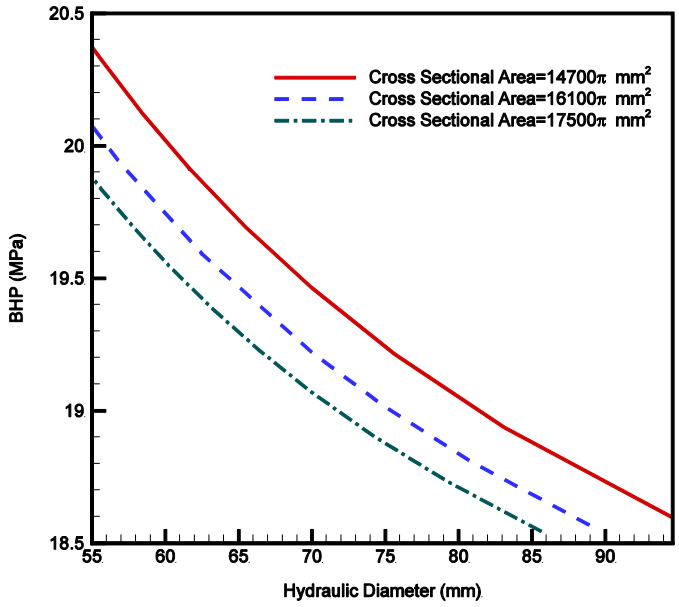

Figure 2. Effects of hydraulic diameter and cross-sectional area on BHP

As Figure (2) shows, for a constant cross-sectional area, by increasing hydraulic diameter, BHP decreased. The variation of BHP versus hydraulic diameter is not linear. Also, the comparison of different charts in figure (2) indicates that by increasing the cross-sectional area, BHP is decreased for a constant hydraulic diameter.

Figure (3) represents the solid volume fraction distribution during the annulus for different hydraulic diameters with a constant cross-sectional area. As this figure shows, in a constant cross-sectional area by increasing hydraulic diameter, the solid volume fraction is decreased during the entire length of the well.

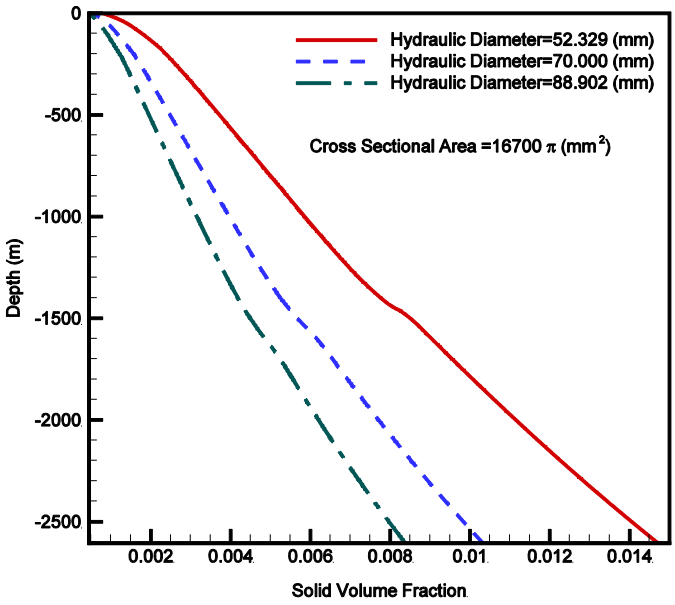

Figure 3. Distribution of solid volume fraction for various hydraulic diameter

Also, figure (4) represents the solid volume fraction distribution during the annulus for the different cross-sectional areas with constant hydraulic diameters. This figure shows that in constant hydraulic diameter, the solid volume fraction is increased by increasing the cross-sectional area.

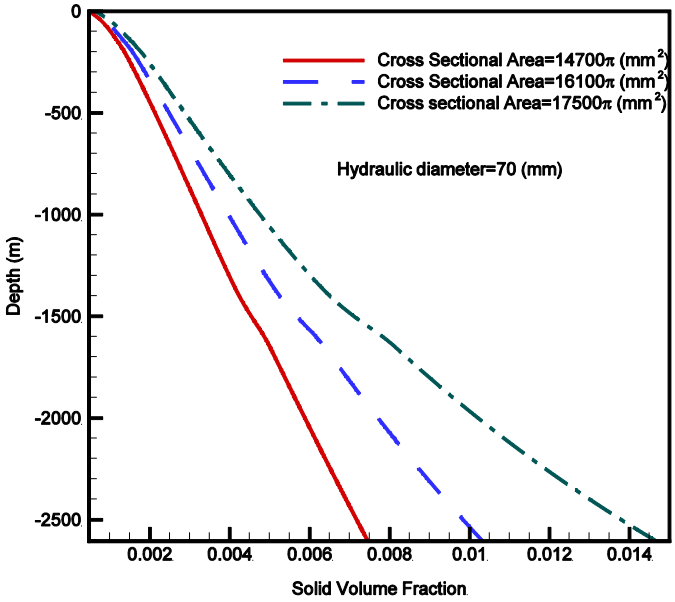

Figure 4. Distribution of solid volume fraction for various cross-sectional area

Effects of liquid properties

During UBD operation, it is the liquid phase that provides the medium which transports the

solid phase (smith et al. [17]). On the other hand, the carrying capacity of a liquid is fully dependent on viscosity. Also, in UBD operation, generally oil-based fluid is used as drilling liquid. Viscosity and density of oil-based liquids are interrelated together. Due to the effects of liquid density on BHP and liquid viscosity on hole-cleaning and dependency of these properties, drilling fluid selection in UBD operation is very important. In this numerical simulation, the viscosity of the liquid phase is calculated as follows (Beggs and Robinson, [18])

$$\mu_{oil} = 0.8115\left(10^{X_{oil}} - 1\right) \tag{13}$$

Where viscosity is in Centipoise (cp), and for X_{oil}, we have

$$X_{oil} = 10^{3.3240 - 0.0203(^{\circ}API)}\left(T^{-1.1630}\right) \tag{14}$$

In the above equations, the temperature is in Fahrenheit (F). The API is an indicator related to specific gravity, and its value, usually varies from 47 for light oil to 10 for heavy oil. API and specific gravity are related together as follows;

$$^{\circ}API = \frac{141.5}{\gamma_{oil}} - 131.5 \tag{15}$$

Figure (5) shows the effects of liquid density variation on Muspac-53 BHP. As this figure shows, increases in the BHP due to increases in the liquid density are not linearly, and the increases are stronger for higher density. Changing the density of the liquid with two different mechanisms affects BHP. Increasing fluid density increases the hydrostatic term of pressure directly. Also, according to the Equations (13)-(15), with changes in liquid density, the liquid's viscosity changes, and this change in viscosity changes the frictional term of the pressure.

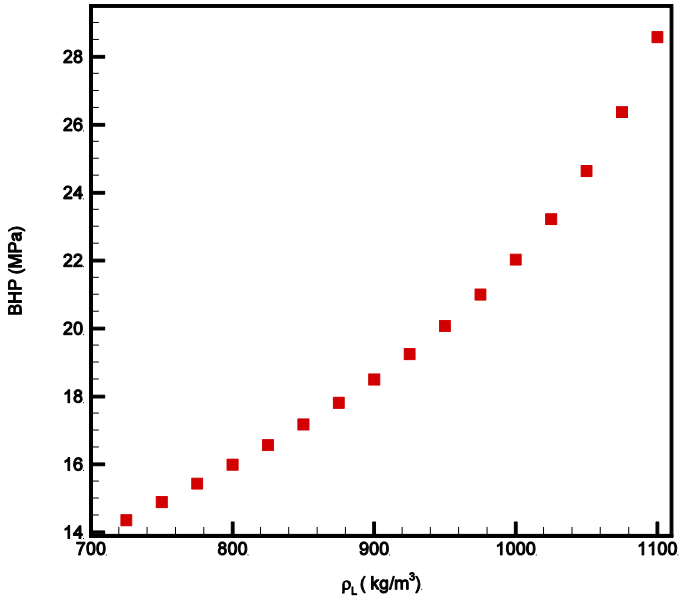

Figure 5. Effects of liquid density on Muspac 53 BHP

The effects of density and so on the effects of viscosity changing on cutting transport are represented in Figure (6). In this figure, the vertical axis represents the ratio of the solid volume fraction at the nearest node after geometry change in the downstream to its value at the nearest node before the geometry change in the upstream for Muspc-53 well in depth of 2555 meters. As this figure shows, increases in liquid density and viscosity, do not always lead to improved hole-cleaning. As seen, the solid volume fraction ratio increases as the density, and so on the viscosity increases until it exhibits a maximum value. After the maximum value, the solid

volume fraction ratio decreases as the viscosity is increased. Increasing the viscosity reduces the velocity of the mixture and increases the cuttings transport capacity. Hence, the curve of solid volume fraction ratio versus density and so on the liquid phase's viscosity is divided into two regions depending on whichever has a dominant effect. On the left-hand side, decreasing the velocity is the dominant factor, and on the right-hand side, increasing the carrying capacity is the dominant factor.

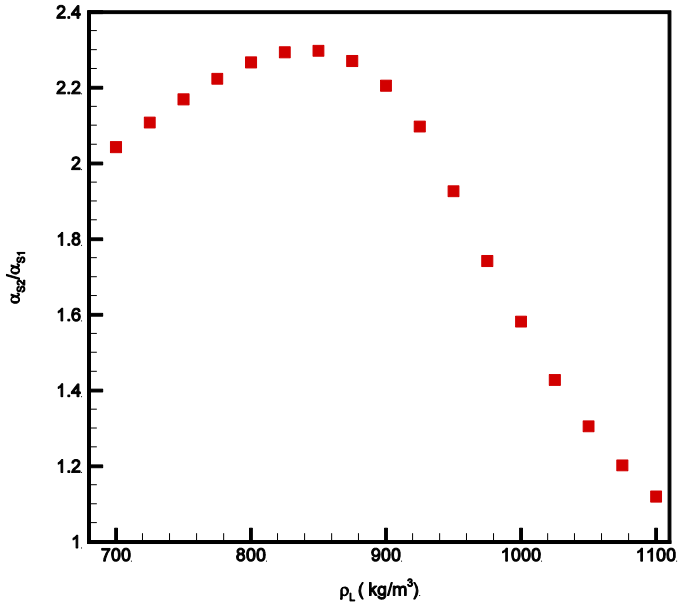

Figure 6. Effects of liquid density on cutting transport in Muspac 53

Conclusions

A numerical procedure based on a one-dimensional multi-fluid model was proposed to simulate gas-liquid-solid three-phase flow in the annulus of real wells during UBD operation. Developed numerical simulation was validated by using two case studies. The effect of hydraulic diameter and cross-sectional area and the effects of liquid density and so on liquid viscosity on BHP and hole-cleaning were investigated numerically. The following conclusions may be drawn:

1- In a constant cross-sectional area, BHP decreased nonlinearly by increasing hydraulic diameter and hole-cleaning improved.

2- In a constant hydraulic diameter, by decreasing the cross-sectional area, BHP increased, and hole-cleaning improved.

3- During UBD operation, by increases of the liquid density and so on increases the liquid viscosity, BHP is increased nonlinearly.

4- The viscosity of the liquid phase affects hole-cleaning through two contrary mechanisms. In fact, as the drilling fluid's viscosity increases, the average velocity of the drilling fluid decreases and causes more cuttings to remain in the annular space. On the other hand, as the drilling fluid's viscosity increases, the carrying capacity of the cuttings by the liquid phase increases, and hole-cleaning improved.

References

[1] Guo B., Hareland G., Rajtar J., 1996, Computer Simulation Predicts Unfavorable Mud Rate and Optimum Air Injection Rate for Aerated Mud Drilling, SPE Drilling & Completion 11 (02): 61-66.

[2] Fan J., Gao C., Taihe S., Liu H., Yu Z., 2001, A comprehensive model and computer simulation for under-balanced drilling in oil and gas wells, Paper SPE 68495 preresented at the SPE/ICoTA Coiled Tubing Roundtable held in Houston, Texas, 7–8 March
[3] Lage A. C. V. M., (Ph.D Dissertation) 2000, Two-Phase Flow Models and Experiments for Low-Head and Underbalanced Drilling, Stavanger University College.
[4] Lage A., Time R., 2002, Experimental and theoretical investigation of upward two-phase flow in annuli, SPE journal 7 (03): 325-336.
[5] Guo B., Ghalambor A., 2002, An innovation in designing under-balanced drilling flow rates: A gas-liquid rate window (GLRW) Approach, Paper SPE 77237 presented at the IADC/SPE Asia Pacific Drilling Technology held in Jakarta, Indonesia, 9–11 September.
[6] Perez-Tellez C. P., (Ph.D. thesis) 2003, Improved Bottom-hole Pressure Control for Underbalanced Drilling Operations. Department of Petroleum Engineering, Louisiana State University.
[7] Perez-Tellez C. P., Smith J. R., Edwards J. K., 2003, A new comprehensive mechanistic model for underbalanced drilling improves wellbore pressure prediction, SPE Drill Completion 18 (3): 199–208.
[8] Fadairo A. S., Adekomaya O., Falode O. A., 2009, Effects of drilling cuttings transport on pressure drop in a flowing well, Paper SPE/IADC 125707 preresented at the Middle East Drilling Technology Conference & Exhibition held in Manama, Bahrain, 26-28 October.
[9] Yan T., Wang K., Sun X., Luan S., Shao S., 2014, State-of-the-art cuttings transport with aerated liquid and foam in complex structure wells, Renewable and Sustainable Energy Reviews 37: 560-568.
[10] Khezrian M., Hajidavalloo E., Shekari Y., 2015, Modeling and simulation of under-balanced drilling operation using two-fluid model of two-phase flow, Chemical Engineering Research and Design 93: 30-37.
[11] Hajidavalloo E., Falavand Jozaei A., Azimi A., Shekari Y., Ghobadpouri S., 2018, Thermal simulation of two-phase flow in under-balanced drilling operation with oil and gas production, Journal of Computational Applied Mechanics 49: 314-322.
[12] Li X., Ma H., Zhao H., Gao D., Lu B., Ding S., Gong D., Ma Z., 2020, Study on the model for predicting maximum allowable measured depth of a horizontal well drilled with underbalanced operation, Journal of Petroleum Science and Engineering 191: 1-8.
[13] Evje S., Flatten T., 2003, Hybrid flux-splitting schemes for a common two-fluid model, Journal of Computational Physics 192 (1): 175-210.
[14] Hatta N., Fujimoto H., Isobe M., Kang J. S., 1998, Theoretical analysis of flow characteristics of multiphase mixtures in a vertical pipe, International Journal of Multiphase Flow 24 (04): 539-561.
[15] Dranchuk P. M., Abu-Kassem J. H., 1975, Calculations of Z-factors for natural gases using equation of state, J. Can. Pet. Technol, 14 (03): 14–34.
[16] Bratland, O., 2010, Pipe Flow 2, Multiphase Flow Assurance. www.drbratland.com.
[17] Smith S., Gregory G., Munro N., Muqeem M., 2000, Application of multiphase flow methods to horizontal underbalanced drilling, Journal of Canadian Petroleum Technology 39 (10): 52-60.
[18] Beggs H. D., Robinson J. R., 1975, Estimating the viscosity of crude oil systems, Journal of Petroleum Technology 27 (09): 1140-1141.